



# $\alpha$ Klotho attenuates cardiac hypertrophy and increases myocardial fibroblast growth factor 21 expression in uremic rats

Paulo Giovanni de Albuquerque Suassuna<sup>1,2</sup> , Paula Marocolo Cherem<sup>1</sup>, Bárbara Bruna de Castro<sup>1</sup>, Edgar Maquigussa<sup>3</sup>, Marco Antonio Cenedeze<sup>3</sup>, Júlio Cesar Moraes Lovisi<sup>2</sup>, Melani Ribeiro Custódio<sup>4</sup>, Helady Sanders-Pinheiro<sup>1,2</sup>  and Rogério Baumgratz de Paula<sup>1,2</sup>

<sup>1</sup>Laboratory of Experimental Nephrology (LABNEX) and Interdisciplinary Nucleus of Laboratory Animal Studies (NIDEAL), Federal University of Juiz de Fora (UFJF), Juiz de Fora, Minas Gerais 36036-900, Brazil; <sup>2</sup>Interdisciplinary Center for Studies, Research and Treatment in Nephrology (NIEPEN), Federal University of Juiz de Fora, Juiz de Fora, Minas Gerais 36036-900, Brazil; <sup>3</sup>Nephrology Division, Department of Medicine, Federal University of São Paulo, São Paulo 04024-002, Brazil; <sup>4</sup>Nephrology Division, Department of Medicine, University of São Paulo, São Paulo 01246-903, Brazil

Corresponding author: Paulo Giovanni de Albuquerque Suassuna. Email: paulosuassuna@gmail.com

## Impact statement

This study aimed to evaluate whether rKlotho replacement can attenuate cardiac remodeling in a post-disease onset therapeutic reasoning and explore the impact on myocardial FGF21 expression. This study contributes significantly to the literature, as the therapeutic effects of rKlotho replacement and FGF21 myocardial expression have not been widely evaluated in a setting of uremic cardiomyopathy. For the first time, it has been demonstrated that subcutaneous rKlotho replacement may attenuate cardiac remodeling in established uremic cardiomyopathy and increase myocardial expression of FGF21, suggesting a correlation between  $\alpha$ Klotho and myocardial FGF21 expression. The possibility of interaction between the  $\alpha$ Klotho and FGF21 cardioprotective pathways needs to be further explored, but, if confirmed, would point to a therapeutic potential of FGF21 in uremic cardiomyopathy.

## Abstract

In chronic kidney disease (CKD), evidence suggests that soluble  $\alpha$ Klotho (sKlotho) has cardioprotective effects. Contrariwise, high circulating levels of fibroblast growth factor 23 (FGF23) are related to uremic cardiomyopathy development. Recently, it has been demonstrated that sKlotho can act as a soluble FGF23 co-receptor, allowing sKlotho to modulate FGF23 actions in the myocardium, leading to the activation of cardioprotective pathways. Fibroblast growth factor 21 (FGF21) is a cardiomyokine with sKlotho-like protective actions and has never been evaluated in uremic cardiomyopathy. Here, we aimed to evaluate whether recombinant  $\alpha$ Klotho (rKlotho) replacement can attenuate cardiac remodeling in an established uremic cardiomyopathy, and to explore its impact on myocardial FGF21 expression. Forty-six male Wistar rats were divided into three groups: control, CKD-untreated, and CKD treated with rKlotho (CKD + KL). CKD was induced by 5/6 nephrectomy. From weeks 4–8, the control and CKD-untreated groups received vehicle, whereas the CKD + KL group received subcutaneous rKlotho replacement (0.01 mg/kg) every 48 h. Myocardial remodeling was evaluated by heart weight/tibia length (HW/TL) ratio, echocardiographic parameters, myocardial histomorphometry, and myocardial expression of  $\beta$ -myosin heavy chain (MHC $\beta$ ), alpha smooth muscle actin ( $\alpha$ SMA), transient receptor potential cation channel 6 (TRPC6), and FGF21. As expected, CKD animals had

reduced levels of sKlotho and increased serum FGF23 levels. Compared to the control group, manifest myocardial remodeling was present in the CKD-untreated group, while it was attenuated in the CKD + KL group. Furthermore, cardiomyocyte diameter and interstitial fibrotic area were reduced in the CKD + KL group compared to the CKD-untreated group. Similarly, rKlotho replacement was associated with reduced myocardial expression of TRPC6, MHC $\beta$ , and  $\alpha$ SMA and a higher expression of FGF21. rKlotho showed cardioprotective effects by attenuating myocardial remodeling and reducing TRPC6 expression. Interestingly, rKlotho replacement was also associated with increased myocardial FGF21 expression, suggesting that an interaction between the two cardioprotective pathways needs to be further explored.

**Keywords:** Chronic kidney disease, uremic cardiomyopathy, Klotho, FGF23, FGF21

*Experimental Biology and Medicine* 2020; 245: 66–78. DOI: 10.1177/1535370219894302

## Introduction

Cardiovascular disease remains the leading cause of mortality in patients with chronic kidney disease (CKD).<sup>1</sup> In these patients, left ventricular hypertrophy (LVH) is the most prevalent cardiac abnormality and is highly correlated with mortality.<sup>2,3</sup> CKD-related LVH represents an underlying cardiomyopathy (termed “uremic cardiomyopathy”) with an unclear multifactorial pathogenesis, characterized not only by cardiomyocyte hypertrophy, but also by exuberant interstitial fibrosis, which leads to mechanical and electrical heart dysfunction.<sup>4,5</sup> Therefore, despite all current advances in dialysis therapy, and hypertension, anemia, and CKD-related mineral and bone disorder (CKD-MBD) treatments, myocardial remodeling continues to occur in CKD patients, resulting in high cardiovascular mortality rates, mainly due to sudden cardiac death.<sup>6</sup>

Recently, phosphate overload, fibroblast growth factor 23 (FGF23) excess, and sKlotho deficiency were shown to play a central role in uremic cardiomyopathy pathophysiology.<sup>7–9</sup> Phosphate retention due to decreased glomerular filtration rate leads to compensatory FGF23 production, resulting in increased phosphate urinary excretion.<sup>10</sup> Consequently, increased circulating FGF23 levels in CKD may be considered an adaptive mechanism for the maintenance of phosphate homeostasis.<sup>11</sup> Faul *et al.*<sup>12</sup> provided evidence supporting the maladaptive effects of FGF23 excess in CKD patients, through its  $\alpha$ Klotho-independent ability to stimulate myocardial type 4 FGF receptor (FGFR4), resulting in calcineurin/NFAT signaling pathway activation, and consequently, cardiac hypertrophy.

Membrane-bound  $\alpha$ Klotho is primarily expressed in the kidney and parathyroid glands, forms complexes with FGFR1–3c and FGFR4, and functions as a FGF23 co-receptor for phosphate homeostasis.<sup>11</sup> Reduced  $\alpha$ Klotho expression has been reported in CKD patients,<sup>13</sup> which may be due to either CKD-induced renal mass loss or  $\alpha$ Klotho expression suppression.<sup>8</sup> The kidneys are supposed to be the main source of circulating sKlotho. Thus, in patients with CKD, sKlotho serum levels are reduced, which correlates with more cardiovascular events and higher mortality.<sup>14,15</sup>

The precise mechanism by which  $\alpha$ Klotho deficiency might contribute to uremic cardiomyopathy development remains unclear. Once membrane-bound  $\alpha$ Klotho is not directly expressed in the heart,<sup>16</sup> its cardioprotective effects must either be indirectly related to its effects in phosphate homeostasis or be mediated by sKlotho.<sup>9,11</sup> sKlotho seems to target several hypertrophic/fibrotic pathways in different cell types, including cardiomyocytes, and exerts numerous pleiotropic protective effects against inflammation, apoptosis, and oxidative stress, resulting in less myocardial hypertrophy and fibrosis.<sup>17–19</sup> Experimentally, while  $\alpha$ Klotho-deficient CKD mice exhibit aggravated cardiac hypertrophy,  $\alpha$ Klotho-overexpressing CKD mice are protected from it.<sup>20</sup> It is well established that sKlotho can prevent heart hypertrophy by inhibiting TRPC6 calcium channels<sup>21,22</sup>; however, it has recently been shown that sKlotho can act as a true circulating co-receptor that binds not only to circulating FGF23, but also to FGF receptors on the cells’ surface,<sup>23</sup> making it possible to modulate

FGF23-mediated signaling, which might trigger some pleiotropic tissue-protective effects of sKlotho.<sup>24</sup>

Similar to FGF23, FGF21 is an endocrine FGF with a Klotho family protein ( $\beta$ Klotho) as co-receptor.<sup>25</sup> Under physiological conditions, FGF21 is produced and secreted primarily by the liver and acts as an endocrine metabolic regulator of glucose and lipid metabolism<sup>26</sup>; however, in pathophysiological scenarios, it can be expressed, secreted, and act locally in different tissues, exerting cytoprotective actions.<sup>27–32</sup> As an autocrine/paracrine factor, FGF21 enhances cell metabolism and increases cellular stress resistance through mitochondrial biogenesis and autophagy enhancement, and activation of anti-oxidation and anti-inflammatory mechanisms.<sup>33,34</sup> Currently, FGF21 is recognized as a protective cardiomyokine with effects resembling those described for sKlotho,<sup>35,36</sup> but there are no data yet on the role of FGF21 in uremic cardiomyopathy. Since Klotho can act as a soluble FGFR1c co-receptor, it can redirect FGF23 action to activation of cardioprotective pathways rather than harmful ones. In this hypothesis, it is reasonable to explore the possibility that one of the protective pathways activated would be the myocardial FGF21 expression.

Here, we aim to evaluate whether rKlotho subcutaneous replacement can, in a post-disease therapeutic approach, attenuate cardiac remodeling in a manner comparable to that observed in previous studies with a preventive approach and, for the first time, explore, in a uremic cardiomyopathy setting, the myocardial expression of FGF21 and the impact of rKlotho replacement on it.

## Materials and methods

### Animals

Forty-six male Wistar rats, aged between 8 and 12 weeks and weighing approximately 250–300 g, were studied. Animals were housed in ventilated cabinets under standard laboratory conditions, with controlled humidity, airflow, temperature of 22 °C  $\pm$  2 °C and 12/12-h light-dark cycle. After weaning, animals were fed with standard feed pellets and water ad libitum. All animal procedures performed in studies were in accordance with institutional ethical standards (IRB approval number 042/2013, 044/2014, 02/2015 e 039/2015 - CEUA-UFJF).

### Experimental model and design

Animals were divided into three groups: control, CKD-untreated, and CKD treated with Klotho (CKD + KL). Uremia was induced in the CKD groups by 5/6 nephrectomy.<sup>37</sup> From four to eight weeks, the control and CKD-untreated groups received vehicle, whereas the CKD + KL group received subcutaneous recombinant  $\alpha$ Klotho replacement (0.01 mg/kg) every 48 h.<sup>22,38</sup> Echocardiogram was performed before protocol initiation and before euthanasia. Animals were kept in metabolic cages for 24-h urine collection a day before euthanasia. For euthanasia, animals were anaesthetized, then the right carotid artery was cannulated for blood pressure measurement and blood sample collection. Immediately after blood collection, the heart was

perfused by ice-cold cardioplegic solution to induce asystolia.<sup>39</sup> The perfused heart was removed; washed; cleaned of fat, pericardium, and atriums; weighed; and then cut at the equatorial cross-section plane into two parts. The apical segment was fractionated and snap-frozen immediately. The remaining heart was fixed in buffered formalin.

### Laboratory measurements

Biochemical analysis was performed for creatinine, urea, calcium, phosphate (serum and urine), and alkaline phosphatase (Cobas c111, Roche®). Creatinine clearance and fractional phosphate excretion were calculated. We measured serum intact parathyroid hormone (PTHi) (Rat Intact PTH (ELISA) Kit, Immotopics, San Clemente, USA), serum FGF23 (Mouse/Rat Intact FGF23 (ELISA) Kit, Immotopics), and serum FGF21 (Quantikine® mouse/rat FGF21 immunoassay, R&D Systems, Minneapolis, USA).  $\alpha$ Klotho measurements were performed by IP-IB assay, as previously described.<sup>13</sup>

### Blood pressure measurement

Blood pressure was measured by carotid artery cannulation with a 24 G polytetrafluorethylene (PTFE) heparinized catheter (Descarpack, Sao Paulo - SP) connected to a pressure transducer (PowerLab® 4/35, ADInstruments Ltd, New South Wales, Australia). The pulse wave was recorded after 5 min for blood pressure stabilization (LabChart® 7.0, ADInstruments Ltd, New South Wales, Australia) and the mean systolic and diastolic blood pressure were calculated.

### Echocardiographic assessment

Echocardiography was performed a day prior to the 5/6th nephrectomy and a day before euthanasia, using a Logiq-e® handheld ultrasound equipment (GE Healthcare, General Electric Company, US) coupled to 18 MHz L8-18i-RS linear hockey stick transducer (GE Healthcare, General Electric Company, US). Pediatric cardiac preset was used for creation of a small animal preset, changing the scale to millimeters and increased scanning speed. Animals were previously sedated with Xylazine 10 mg/kg intraperitoneal injection and Fentanyl 0.025 mg/kg intramuscular injection.

Interventricular septum and left ventricular posterior wall thickness, as well as left ventricular dimensions were obtained by two-dimensional targeted M-mode echocardiographic images at the tips of the papillary muscle from the parasternal short- and long-axis views. Left atrium (LA) was measured in the parasternal long-axis view, just before the mitral valve opening. Transmitral early (E) and late (A) flow velocities were measured by Doppler technique with the sample volume placed at the tips of the mitral leaflet in apical 4-chamber view. Doppler tissue signals (E' and A' velocities) were obtained at the base of the interventricular septum.

### Morphological analysis

After the heart was removed and cleaned of fat, pericardium, and atriums, it was weighed and the HW/TL ratio was calculated, fixed in buffered formalin, and then embedded

in paraffin. Four micron cardiac sections in the equatorial plane, including both ventricles, were stained with hematoxylin-eosin (HE) and Picrosirius red (PS), to estimate cardiomyocyte hypertrophy and collagen volume fraction, respectively, using a previously published protocol.<sup>40</sup> The digital image system Axio Cam 506c - Axiovision 4.9.1 software (Carl Zeiss Microscopy, LLC, US) and ImageJ software (National Institutes of Health, EUA) were used for image acquisition and morphometric measurements, respectively.

### Immunohistochemistry

Heart slices were deparaffinized and rehydrated, then processed for antigens retrieval, blockade of endogenous peroxidase activity, and non-specific binding sites. Sections were incubated overnight at 4°C with the following (presented as primary antibodies/dilution): anti-MHC $\beta$ /1:800 (MYH7 Monoclonal Antibody - TH81, Thermo Fisher Scientific, Rockford, IL, USA), anti- $\alpha$ SMA/1:800 (Smooth Muscle Actin Monoclonal Antibody (1A4asm-1), Thermo Fisher Scientific), and anti-TRPC6-extracellular ACC-120/1:250 (Alomone Labs, Jerusalem, Israel). Antibody-antigen binding sites were revealed with 3,3'-Diaminobenzidine (DAB). Image acquisition was performed using light microscopy (Axiophot HBO50, Carl Zeiss, Goettingen, Germany) equipped with a high-resolution digital image system (AmScope camera MU100, United Scope LLC, California, USA). Captures consisted of 10 consecutive and non-overlapping fields, covering the entire LV circumference at 200 $\times$  magnification. In each field, the area stained with DAB was estimated using ImageJ software version 1.52h (National Institutes of Health, USA) according to a previously described technique.<sup>41</sup>

### Western blot analysis

Heart fragments were homogenized in ice-cold lysis buffer containing protease inhibitors (AEBSF-Protease Inhibitor Cocktail; Sigma Aldrich). Fifty-microgram protein samples were separated according to size by 12% sodium dodecyl sulfate-polyacrylamide gel electrophoresis (SDS-PAGE) and electroblotted onto nitrocellulose membranes. Membrane blots were probed with anti-FGF21 1:1000

**Table 1.** Biochemical and hormonal parameters in the 8th week of experiment.

Variable	Control	CKD	CKD + KL
Creatinine (mg/dL)	0.27 $\pm$ 0.04	0.58 $\pm$ 0.07*	0.62 $\pm$ 0.06*
Urea (mg/dL)	41.5 $\pm$ 4.7	80.2 $\pm$ 14.1*	90.6 $\pm$ 14.2*
CrCl (ml/min/100 g)	2.09 $\pm$ 0.55	1.13 $\pm$ 0.17*	1.01 $\pm$ 0.13*
Calcium (mg/dL)	8.6 $\pm$ 0.3	9.2 $\pm$ 0.2	9.2 $\pm$ 0.4
Alkaline phosphatase (U/L)	104.3 $\pm$ 18.0	116.3 $\pm$ 14.1	117.2 $\pm$ 12.5
Phosphate (mg/dL)	6.1 $\pm$ 0.7	6.3 $\pm$ 0.8	6.4 $\pm$ 12.5
FPe (%)	8.96 $\pm$ 1.65	20.08 $\pm$ 3.88*	24.28 $\pm$ 5.30*
PTHi ( $\mu$ g/mL)	464.8 $\pm$ 115.1	1059.0 $\pm$ 315.3*	1113.0 $\pm$ 353.9*
FGF23 ( $\mu$ g/mL)	129.9 $\pm$ 28.7	208.8 $\pm$ 33.9*	200.5 $\pm$ 32.0*
$\alpha$ Klotho ( $\rho$ M)	188.4 $\pm$ 29.7	36.18 $\pm$ 21.38*	49.26 $\pm$ 25.6*

Note: Values expressed as mean  $\pm$  SD and ANOVA and Tukey tests used to compare groups \* $P$  < 0.05 compared to control group.

(Invitrogen, PA5-44325) overnight at 4°C and with horse-radish peroxidase (HRP)-conjugated secondary antibodies for 1 h at 4°C. Protein bands were visualized using the Immobilon Western HRP substrate (Millipore), and

quantified using Uvitec analyses software (Uvitec Limited, Cambridge, UK) as previously described.<sup>42</sup> Ponceau staining was used as a loading control as previously described.<sup>43</sup>

### Systolic and diastolic blood pressures

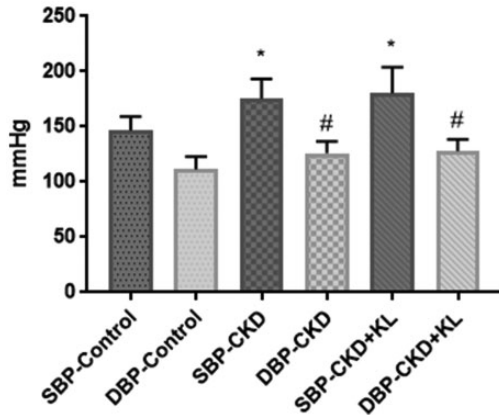


**Figure 1.** Blood pressure levels measured by carotid puncture on the day of euthanasia. SBP: systolic blood pressure; DBP: diastolic blood pressure; CKD: chronic kidney disease group; CKD + KL: klotho-treated chronic kidney disease group. Values expressed as mean  $\pm$  SD and ANOVA and Tukey tests used to compare groups. \*, # $P < 0.05$  compared to control group.

### Quantitative polymerase chain reaction

Total RNA was extracted from snap-frozen myocardium by the phenol-guanine isothiocyanate-cesium chloride methods as previously described.<sup>44</sup> Expression of specific mRNA sequences (TRPC6 (Rn00677559\_m1), FGF-21 (Rn00590706\_m1),  $\beta$ MHC (Rn00691731\_m1),  $\alpha$ MHC (Rn00691721\_g1), and Acta2 (Rn01759928\_g1)) was assessed by quantitative polymerase chain reaction (PCR) using published protocols.<sup>45</sup> Gene expression was normalized by an internal control gene HPRT (Mn00443358\_m1).

### Statistical analysis

Data normality was assessed by the Shapiro-Wilk test. Comparison between all groups was performed with one-way analysis of variance, followed by Tukey's *post hoc* test. Results are expressed as mean  $\pm$  SD (standard deviation) at a significance level of  $P < 0.05$ . All statistical analyses were carried out using SPSS 22

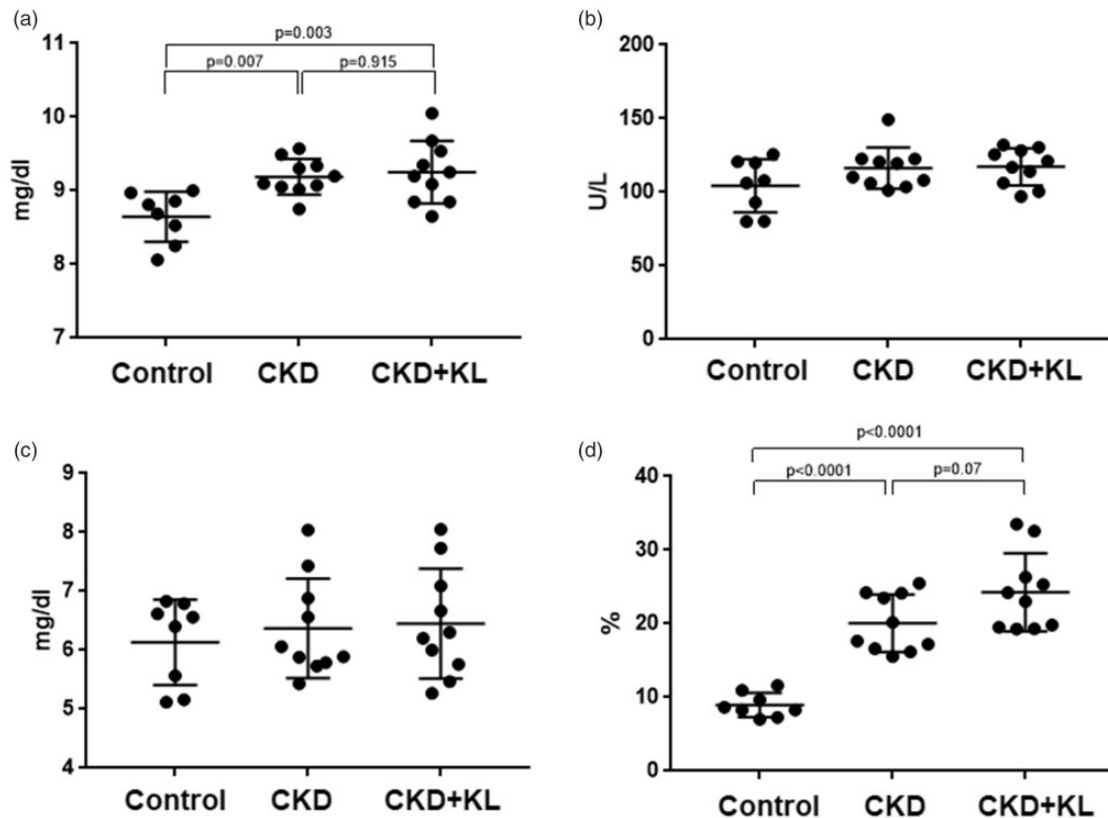


**Figure 2.** Biochemical parameters related to mineral and bone metabolism (serum), evaluated at the 8th week after 5/6 nephrectomy. Results presented as scatter plots (sample size, median and IQR) and compared by ANOVA and Tukey tests. (a) Calcium, (b) Alkaline phosphatase, (c) Phosphate, (d) Fractional phosphate excretion. CKD: chronic kidney disease group; CKD + KL: klotho-treated chronic kidney disease group.

(IBM Corporation, Chicago, IL, USA) and Prism 7 (GraphPad, San Diego, CA, USA).

## Results

### Renal function, blood pressure, and mineral and bone profile

The 5/6 nephrectomy resulted in an average reduction of 50% in the glomerular filtration rate as shown by increased serum creatinine and reduced creatinine clearance. The degree of resulting renal dysfunction was equivalent to category 3 CKD in humans. There was no difference in renal function between CKD groups (Table 1). CKD animals presented higher systolic and diastolic pressure levels than controls. However, systolic or diastolic blood pressure did not differ between CKD-untreated and CKD + KL groups (Figure 1). Moreover, renal function loss affected mineral and bone metabolism, resulting in increased fractional phosphate excretion (FPe), PTHi, and FGF23, and decreased serum  $\alpha$ Klotho levels. No significant changes were observed in serum phosphate or alkaline phosphatase levels (Table 1, Figures 2 and 3).

### Echocardiographic assessment

Echocardiographic evaluation showed a significant LVH in the CKD-untreated group compared to the control group, considering interventricular septum thickness, LV posterior wall thickness, and LV mass. In the CKD + KL group, echocardiographic parameters were significantly reduced, and no significant difference was observed in relation to the control group. No changes in LV systolic function were observed among all groups, when assessed by LV fractional shortening (FS-VE) and LV ejection fraction (FE-VE). Diastolic function assessment showed that both left atrium diameter and E/E' ratio were significantly higher, whereas the E'/A' ratio was significantly lower in the CKD group than in the control group. Thus, left atrial enlargement in CKD animals suggests a higher LV filling pressure, whereas the reduced E'/A' ratio and increased E/E' ratio might indicate lower LV compliance (Table 2).

### Myocardial remodeling assessment by HW and histomorphometry

A higher HW/TL ratio was observed in the CKD-untreated group than in the control and CKD + KL groups (Figure 4 (a)). Confirming the echocardiographic findings, a thicker

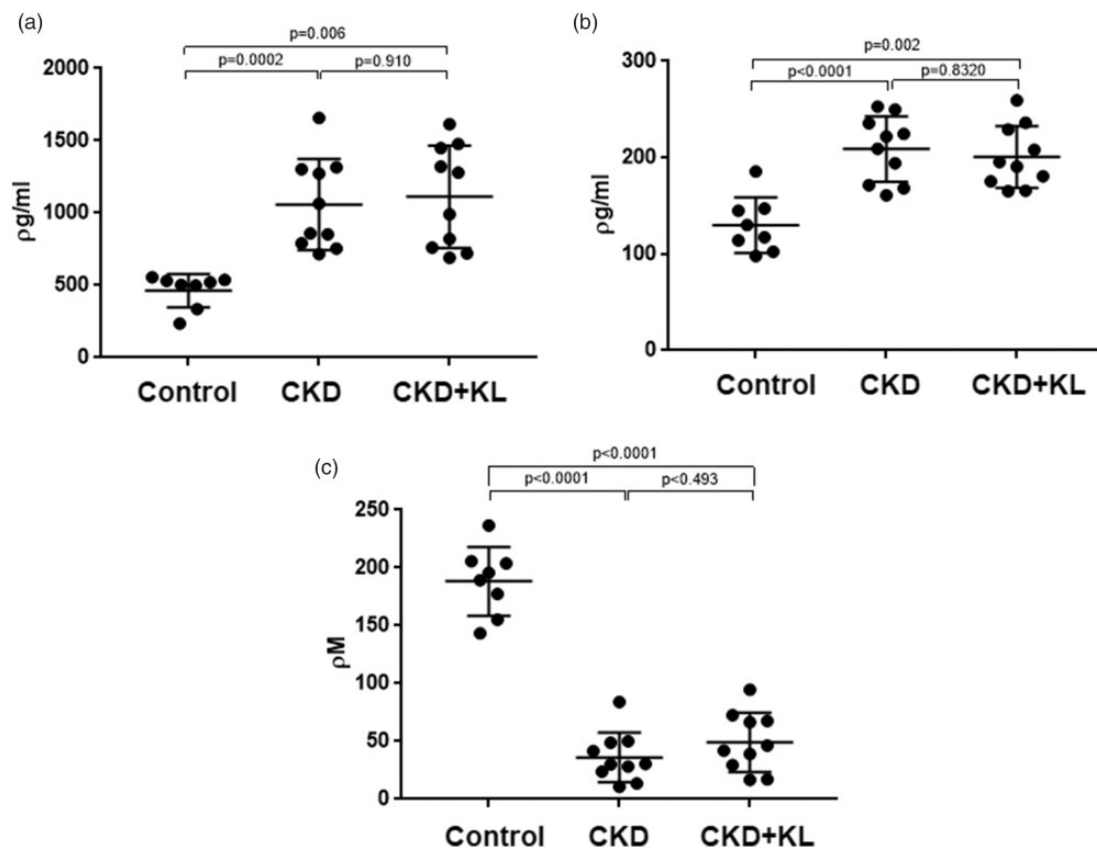


**Figure 3.** Hormonal parameters related to mineral and bone metabolism (serum), evaluated at the 8th week after 5/6 nephrectomy. Results presented as scatter plots (sample size, median and IQR) and compared by ANOVA and Tukey tests. (a) PTHi, (b) FGF23i, (c)  $\alpha$ Klotho. CKD: chronic kidney disease group; CKD + KL: klotho-treated chronic kidney disease group.

interventricular septum was observed by direct measurement of the cardiac sections of the CKD-untreated group (Figure 4(b) and (c)). Histomorphometry assessment showed a significant increase in cardiomyocyte diameter and interstitial fibrosis amount in the CKD-untreated

group, whereas in the CKD + KL group, these parameters were attenuated (Figure 5).

**Table 2.** Echocardiographic parameters, evaluated at the 8th week after 5/6 nephrectomy.

Parameter	Control	CKD	CKD + KL
IVSd (mm)	1.41 ± 0.10	1.58 ± 0.11*	1.42 ± 0.10
LVPWd (mm)	1.45 ± 0.07	1.54 ± 0.09*	1.42 ± 0.08
LVEDd (mm)	8.02 ± 0.62	7.75 ± 0.62	7.89 ± 0.32
LVESd (mm)	4.79 ± 0.46	4.74 ± 0.55	4.71 ± 0.18
LV Mass (mg)	736.5 ± 123.4	883.1 ± 128.4*	750.4 ± 114.8
FS-LV (%)	40.23 ± 2.47	38.87 ± 2.89	40.40 ± 2.04
EF-LV (%)	76.16 ± 2.81	73.48 ± 3.63	76.41 ± 2.19
Left atrium (mm)	4.72 ± 0.54	5.81 ± 0.46 <sup>#</sup>	5.49 ± 0.56 <sup>#</sup>
E/A	2.29 ± 0.42	2.02 ± 0.35	2.08 ± 0.36
E'/A'	3.20 ± 0.84	2.11 ± 0.39 <sup>#</sup>	2.02 ± 0.52 <sup>#</sup>
E/E'	2.56 ± 0.69	3.48 ± 0.80 <sup>#</sup>	3.81 ± 0.69 <sup>#</sup>

\* $P < 0.05$  compared to the control and CKD + KL groups. <sup>#</sup> $P < 0.05$  in the comparison of the control group with the CKD and CKD + KL groups. Note: Values expressed as mean ± SD and compared by ANOVA and Tukey tests.

CKD: chronic kidney disease group; CKD + KL: klotho-treated chronic kidney disease group; IVSd: diastolic interventricular septum thickness; LVPWd: diastolic left ventricular posterior wall thickness; LVEDd: left ventricular end-diastolic diameter; LVESd: left ventricular end-systolic diameter; LV mass: left ventricular mass; FS-LV: left ventricular fractional shortening; EF-LV: left ventricular ejection fraction.

### Myocardial remodeling assessment by hypertrophy and fibrosis marker expression

For myocardial hypertrophy markers, we evaluated  $\beta$ - and  $\alpha$ -myosin heavy chain ( $\beta$ MHC and  $\alpha$ MHC) expressions. In myocardial remodeling, there was increased  $\beta$ MHC and reduced  $\alpha$ MHC expressions. Accordingly, a significant increase was noted in myocardial  $\beta$ MHC expression in the CKD-untreated group at both mRNA and protein levels. Conversely,  $\beta$ MHC expression was attenuated in the CKD + KL group compared to the CKD-untreated group (Figure 6(a) and (b)). The  $\alpha$ MHC/ $\beta$ MHC ratio was evaluated at the mRNA level by qRT-PCR, and a significant reduction in this ratio was observed in the CKD-untreated group compared to the control group, whereas a partial recovery was detected in the CKD + KL group (Figure 6(c)).

As a myocardial fibrosis marker, tissue expression of alpha smooth muscle actin ( $\alpha$ SMA) was assessed by IHC and qRT-PCR. Myocardial  $\alpha$ SMA expression is very low under normal conditions, but its expression increases during remodeling, especially during myofibroblast onset. Therefore, a significant increase in  $\alpha$ SMA expression both at mRNA and protein levels was detected in the CKD-untreated group, greater than in the control group.

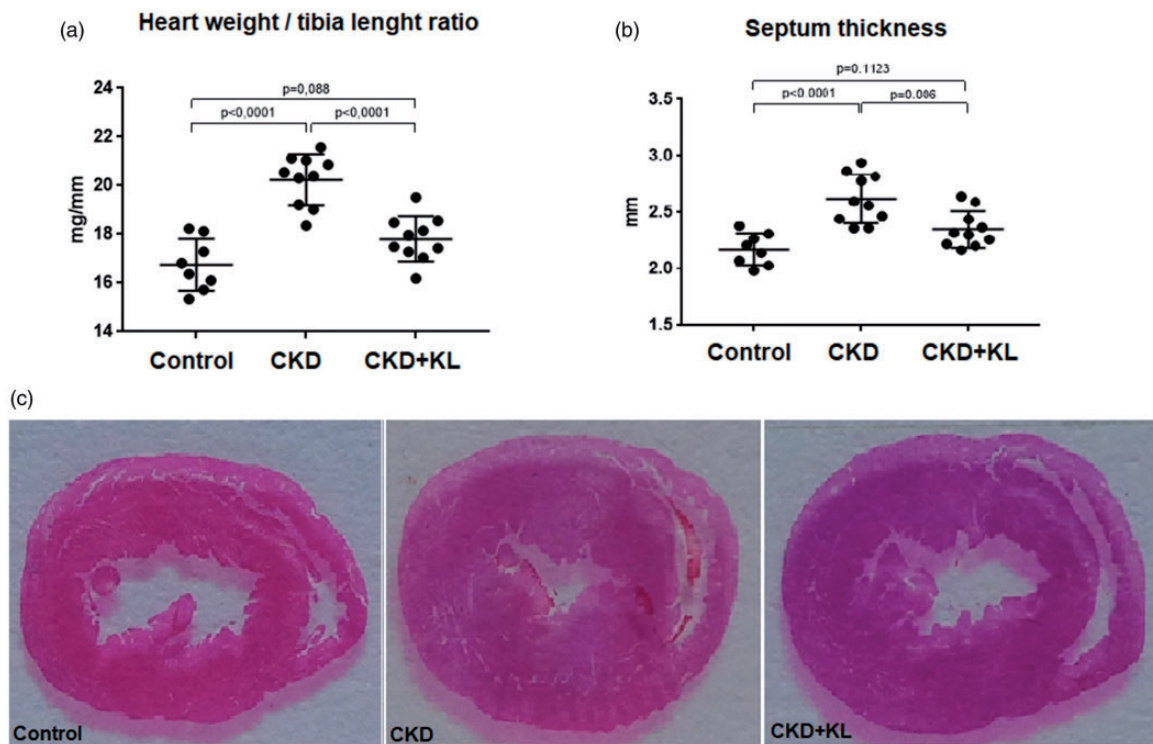


**Figure 4.** Evaluation of cardiac remodeling. (a) Heart weight/tibia length and (b) direct measurement of interventricular septum thickness. (c) Illustrative photos of cross sections of the heart at equatorial level and stained with H & E, 100 $\times$ . Results presented as scatter plots (sample size, median and IQR) and compared by ANOVA and Tukey tests. CKD: chronic kidney disease group;

CKD + KL: klotho-treated chronic kidney disease group. (A color version of this figure is available in the online journal.)

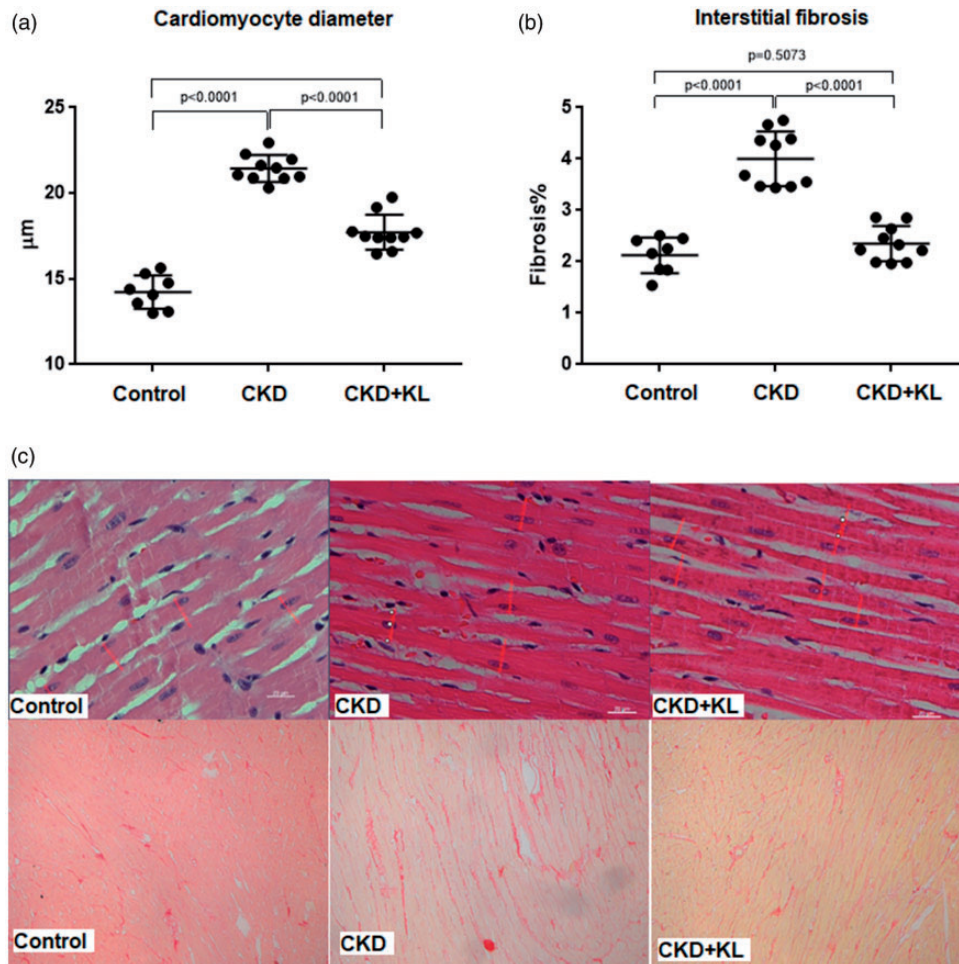


**Figure 5.** Evaluation of myocardial remodeling by histomorphometry: (a) Measurement of cardiomyocytes diameter and (b) Interstitial fibrosis area. (c) Illustrative photos of myocardial tissue in H & E stains, 400 $\times$  and Picrosirius, 200 $\times$ . Results presented as scatter plots (sample size, median and IQR) and compared by ANOVA and Tukey tests.

CKD: chronic kidney disease group; CKD + KL: klotho-treated chronic kidney disease group. (A color version of this figure is available in the online journal.)

However, in the CKD + KL group,  $\alpha$ SMA expression returned to baseline levels (Figure 7).

We also appraised myocardial expression of the cationic channel TRPC6. A significant increase in mRNA expression was observed in both CKD groups, more than in the control group. However, cardiomyocyte transmembrane-TRPC6 expression, addressed by IHC using an antibody against extracellular TRPC6, was significantly increased in the myocardium of the CKD-untreated group, whereas the CKD + KL group had attenuation of its membrane expression (Figure 8).

### Serum FGF21 levels and its myocardial expression

A significant increase of serum FGF21 levels was detected in the CKD groups than in the control group (Figure 9). Likewise, myocardial FGF21 expression, both at mRNA and protein levels, was significantly increased in the CKD groups than in the controls. However, compared to the CKD-untreated group, the CKD + KL group had higher myocardial FGF21 expression at mRNA and protein levels, suggesting an influence of rKlotho replacement (Figure 9).

## Discussion

Our results demonstrated that subcutaneous rKlotho replacement showed a cardioprotective effect in a post-disease onset therapeutic reasoning, since it was able to attenuate the CKD-induced hypertrophy and myocardial fibrosis. The mechanisms by which this endocrine factor exerts its protective effects on myocardium are still unclear, but rKlotho replacement reduced tissue expression of myocardial hypertrophy and fibrosis markers and decreased cardiomyocyte membrane expression of TRPC6. Moreover, for the first time, we found a possible correlation between rKlotho replacement and increased myocardial FGF21 expression, suggesting that FGF21, as a protective cardiomyokine, may be responsible for some cardioprotective effects attributed to sKlotho.

Although no sKlotho receptor has yet been described, a direct cardioprotective effect of sKlotho is well established by many *in vitro* studies. These studies with isolated cardiomyocytes have reported the direct cardioprotective effect of sKlotho by interfering in several hypertrophic and fibrotic pathways, such as the TRPC6 cardiomyocyte membrane expression, AT1/AII, TGF $\beta$ , and Wnt/ $\beta$ -Catenin pathways,

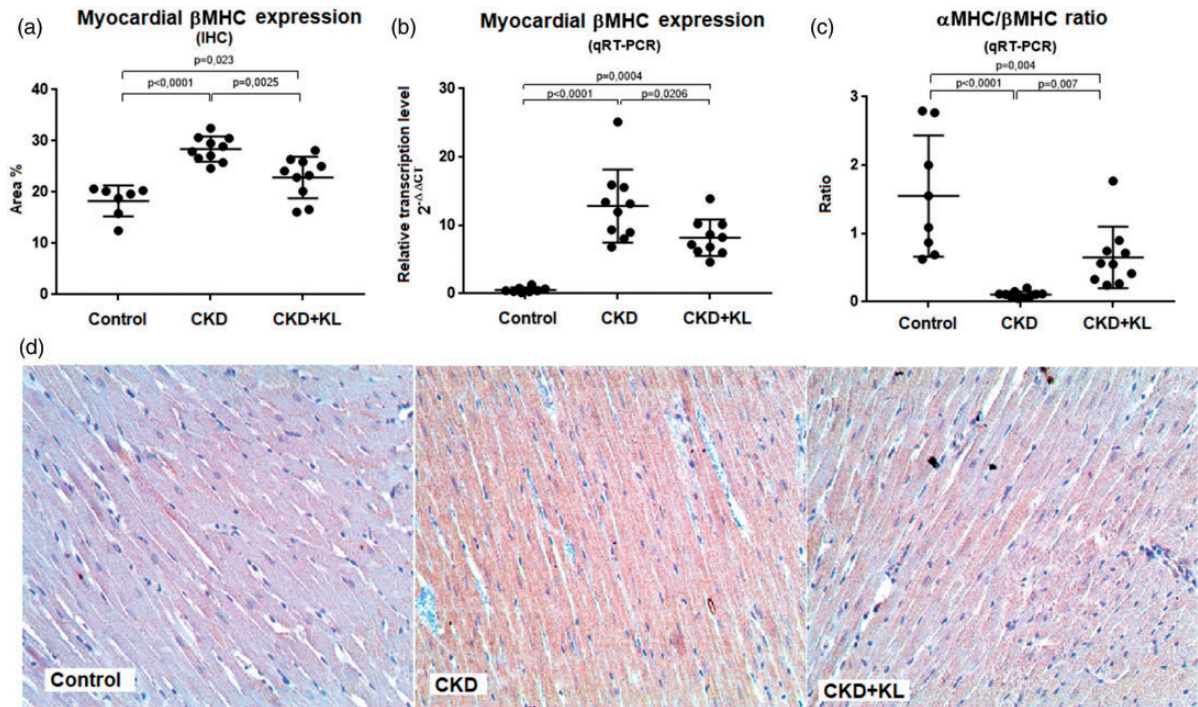


**Figure 6.** Evaluation of myocardial remodeling through the tissue expression of  $\beta$ MHC and the  $\alpha$ MHC/ $\beta$ MHC ratio. (a) Expression of  $\beta$ MHC quantified by IHC and (b) by qRT-PCR. (c) Ratio of mRNA expression between  $\alpha$ MHC and  $\beta$ MHC. (d) Illustrative myocardial photos with IHC with anti- $\beta$ MHC + DAB, 200 $\times$ . Results presented as scatter plots (sample size, median and IQR) and compared by ANOVA and Tukey tests.

CKD: chronic kidney disease group; CKD + KL: klotho-treated chronic kidney disease group. (A color version of this figure is available in the online journal.)

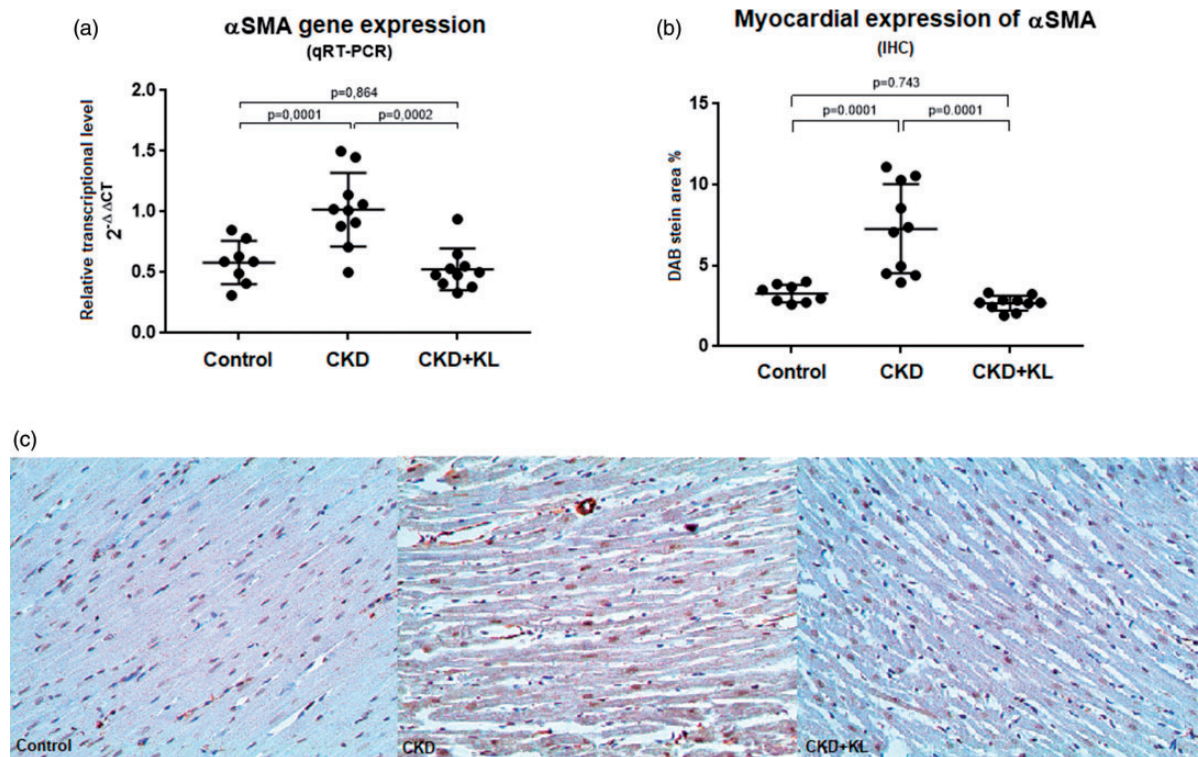


**Figure 7.** Evaluation of myocardial alpha-smooth muscle actin ( $\alpha$ SMA) expression. (a) Area occupied by  $\alpha$ SMA evaluated by immunohistochemistry (IHC). (b) Relative  $\alpha$ SMA mRNA expression by qRT-PCR. (c) Illustrative photos of myocardial tissue with IHC with anti- $\alpha$ SMA + DAB, 200 $\times$ . Results presented as scatter plots (sample size, median and IQR) and compared by ANOVA and Tukey tests.

CKD: chronic kidney disease group; CKD + KL: klotho-treated chronic kidney disease group. (A color version of this figure is available in the online journal.)



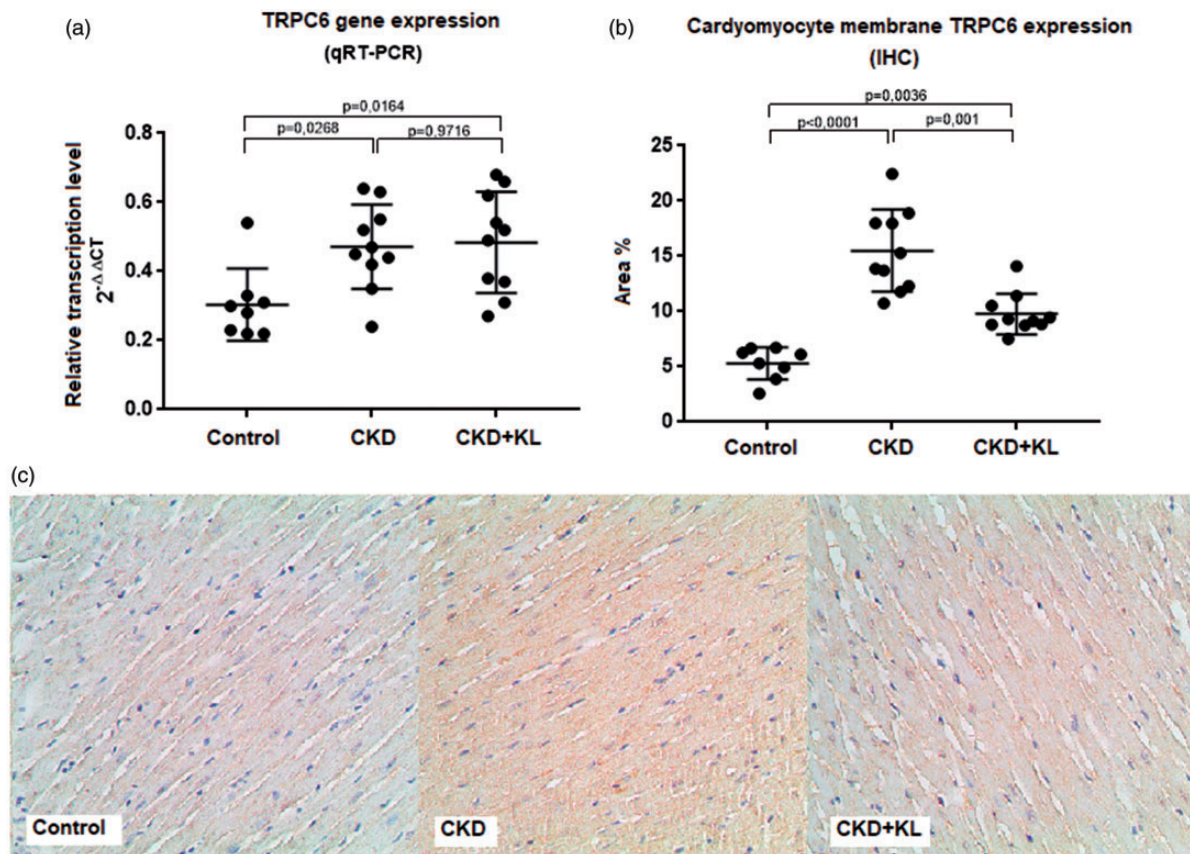


**Figure 8.** Evaluation of myocardial transient receptor potential cation channel 6 (TRPC6) expression. (a) Evaluation by immunohistochemistry (IHC) of cardiomyocyte membrane TRPC6 cation channels expression. (b) Relative TRPC6 mRNA expression. (c) Illustrative photos of myocardial tissue with IHC with extracellular anti-TRPC6 + DAB, 200 $\times$ . Results presented as scatter plots (sample size, median and IQR) and compared by ANOVA and Tukey tests. CKD: chronic kidney disease group; CKD + KL: klotho-treated chronic kidney disease group. (A color version of this figure is available in the online journal.)

and attenuating noxious stimuli, such as oxidative stress and inflammation.<sup>20–22,46–48</sup> *In vivo* studies reported that Klotho deficiency is detrimental to the heart, whereas its abundance is protective. Thus, heterozygous  $\alpha$ Klotho-deficient mice are prone to develop intense cardiac hypertrophy and fibrosis in both stress-induced (isoprenaline) and uremic cardiomyopathy models.<sup>22,48</sup> Conversely, transgenic  $\alpha$ Klotho-overexpressing mice are protected from cardiac hypertrophy and fibrosis. In these *in vivo* studies, animals exhibit a primary deficiency or abundance of  $\alpha$ Klotho. Likewise, early intraperitoneal rKlotho administration was shown to protect against cardiac pathological changes in mice injected with isoprenaline or indoxyl sulphate.<sup>22,48</sup> All these studies demonstrated a preventive effect of sKlotho against cardiac remodeling in different scenarios. However, data on the efficacy of late rKlotho treatment for uremic cardiomyopathy are lacking.

In our study, we sought a therapeutic approach. The rKlotho replacement treatment was started after a four-week disease progression period to mimic the events in CKD patients. In addition to the therapeutic approach, we modified the rKlotho replacement route from IP to the subcutaneous route, since this is routinely used for peptide hormone replacement in clinical practice and might increase rKlotho bioavailability.<sup>49</sup> Our results robustly demonstrated that rKlotho treatment attenuated

myocardial remodeling by decreasing echocardiographic, histological, and molecular remodeling parameters in the CKD + KL group, compared to the CKD-untreated group, suggesting its potential in uremic cardiomyopathy treatment.

As reference of sKlotho cardioprotective effects, myocardial expression of TRPC6 was evaluated. The cationic channel TRPC6 acts as a mechanical stress sensor of cardiomyocyte walls, increasing intracellular calcium influx and activating hypertrophy-related signaling pathways, specifically the calcineurin/NFAT pathway.<sup>50–52</sup> TRPC6 expression is increased in several experimental models of cardiac hypertrophy and its reduction offers protection. Consistent with Xie *et al.*'s findings in mice with  $\alpha$ Klotho overexpression, treatment of an established uremic cardiomyopathy with rKlotho reduced cardiomyocyte membrane TRPC6 expression, despite its higher myocardial expression at the mRNA level induced by CKD. The mechanism by which sKlotho modulates TRPC6 cation channel localization has recently been elucidated. sKlotho is able to bind to monosialogangliosides present on cell membrane lipid rafts, modulating its lipid organization and resulting in TRPC6 externalization inhibition.<sup>53</sup>

For the first time, myocardial FGF21 expression was explored in a scenario of uremic cardiomyopathy, as well as the effect of rKlotho replacement on it. Beyond the

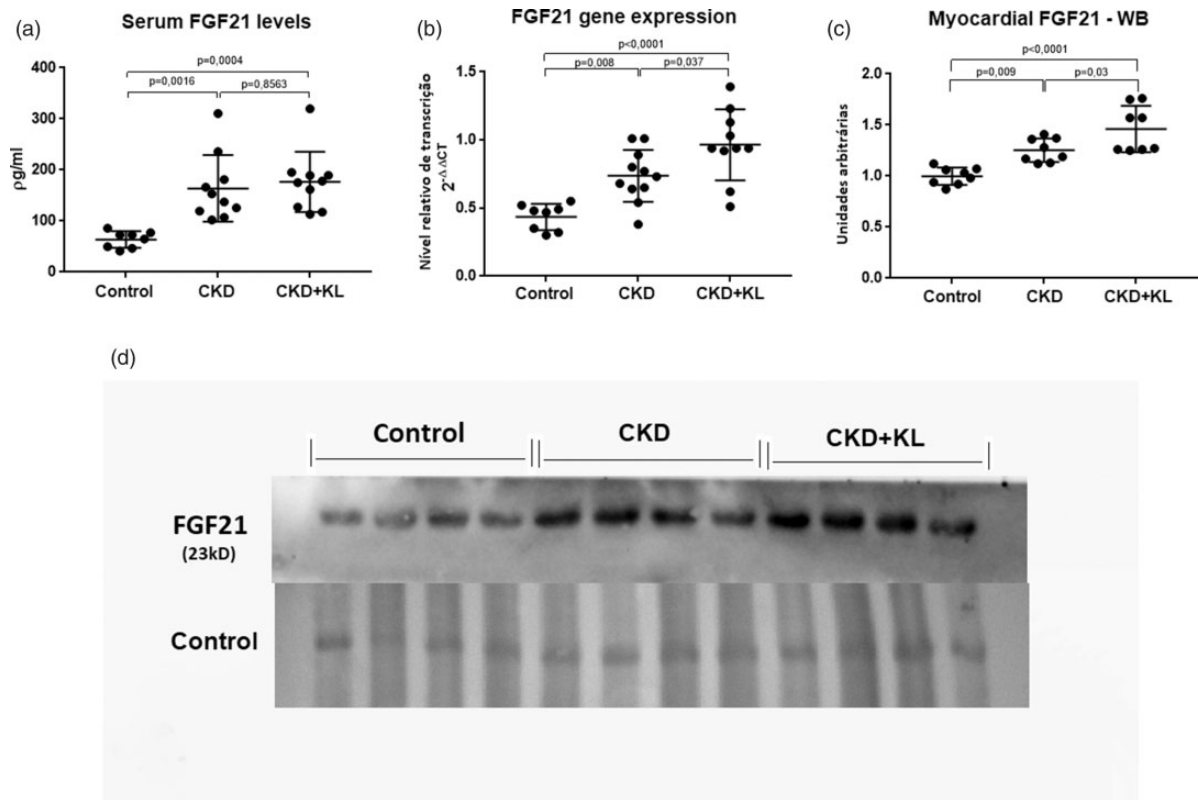


**Figure 9.** Evaluation of serum levels and myocardial expression of FGF21. (a) Serum levels; (b) Protein expression by WB; (c) Expression at the mRNA level by qRT-PCR; (d) Illustrative picture of WB quantification. Results presented as scatter plots (sample size, median, and IQR) and compared by ANOVA and Tukey tests. CKD: chronic kidney disease group; CKD + KL: klotho-treated chronic kidney disease group.

hormonal effects on glucose and lipid metabolism, FGF21 presents cytoprotective actions and participates in the cellular stress response.<sup>33,54,55</sup> Additionally, FGF21 has recently been recognized as a protective cardiomyokine.<sup>36</sup> Therefore, FGF21 knockout mice, when exposed to cardiac stress by different mechanisms, develop worse cardiac remodeling than wild-type animals. Contrarily, animals under FGF21 replacement exhibit attenuated remodeling.<sup>27,36,56</sup> Thus, the myocardium in different scenarios of cellular stress can secrete FGF21 that acts in an autocrine/paracrine manner, increasing the metabolic capacity of cardiomyocytes and reducing oxidative stress, inflammatory pathways, and apoptosis.<sup>35</sup> These cytoprotective actions reported for FGF21 are similar to those induced by  $\alpha$ Klotho replacement,<sup>54,57–60</sup> and it is plausible to speculate that some cytoprotective effects attributed to  $\alpha$ Klotho may be mediated by the increased myocardial FGF21 expression.

In support of this hypothesis, we observed that, although myocardial FGF21 expression was increased in all CKD animals compared to controls, this increase was significantly higher in the CKD + KL group. Increased myocardial FGF21 expression in CKD animals was expected due to increased uremia and hypertension-induced cardiac stress. However, significantly higher expression in the CKD + KL group than in the untreated CKD group may allude to a connection between rKlotho supplementation and myocardial FGF21 expression. Regarding serum levels of FGF21, all CKD animals also

showed higher levels compared to controls, but in a similar range. Since systemic levels of FGF21 are mainly dependent on their production by the liver and renal clearance rate,<sup>26,61</sup> elevated systemic levels were expected after renal function loss.<sup>62</sup> The fact that increased myocardial FGF21 expression after rKlotho treatment was not accompanied by a simultaneous increase in serum FGF21 levels beyond what was expected, suggests that rKlotho action occurred only locally in the myocardium and not systemically.

The deleterious effect of FGF23 on the myocardium occurs through  $\alpha$ Klotho-independent activation of FGFR4 that triggers intracellular signaling via the PLC $\gamma$ /calci-neurin/NFAT pathway, leading to pathologic myocardial hypertrophy and fibrosis.<sup>12,60</sup> The current understanding that sKlotho has an affinity for circulating FGF23, as well as that it may act as a soluble co-receptor for cell surface FGF receptors, allows us to suppose that sKlotho could modulate myocardial FGF23 actions by two distinct mechanisms: first by blocking the binding of circulating FGF23 to the FGFR4 on cardiomyocyte membrane and, secondly, serving as a co-receptor for FGFR1c, which could redirect the action of FGF23 to activation of the cardioprotective pathways rather than the detrimental ones.<sup>24</sup> In this hypothesis, it makes sense to explore the possibility that one of the protective pathways activated would be the myocardial FGF21 expression (Figure 10).

The effect of FGF23 binding to myocardial sKlotho-FGFR1c complex is unknown, but it could result in

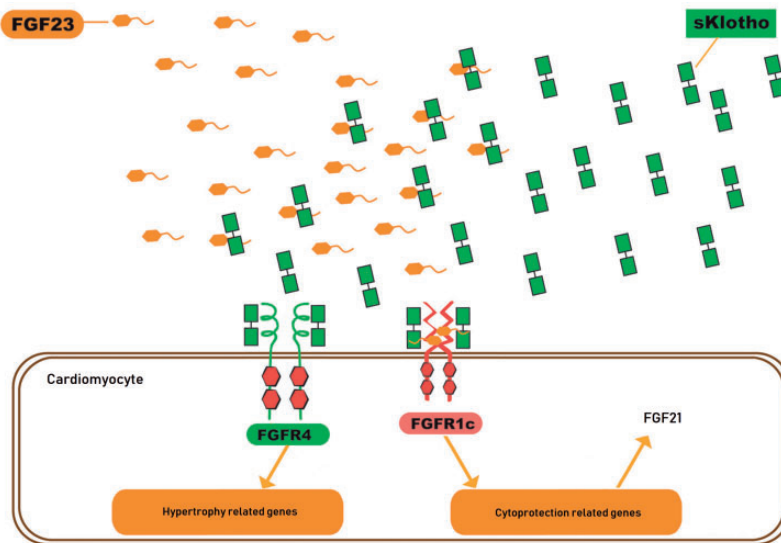


**Figure 10.** Hypothetical mechanism by which sKlotho could increase FGF21 expression. Currently, it is believed that sKlotho has affinity for circulating FGF23 and can act as a soluble co-receptor for cell surface FGF receptors. This action allows us to hypothesize that sKlotho might modulate myocardial FGF23 actions by two distinct mechanisms: first by blocking the binding of circulating FGF23 to the FGFR4 on cardiomyocyte membrane and, secondly, serving as a co-receptor for FGFR1c, which could redirect the action of FGF23 to activation of the cardioprotective pathways rather than the detrimental ones. In this hypothesis, it makes sense to explore the possibility that one of the protective pathways activated would be the myocardial FGF21 expression. (A color version of this figure is available in the online journal.)

FRS2 $\alpha$ -dependent pathway activation (ERK1/2 and Akt signaling pathways).<sup>11</sup> Unlike the calcineurin/NFAT pathway, signaling through ERK1/2 and Akt pathways is associated with physiological cardiac hypertrophy, such as secondary to physical activity or pregnancy.<sup>63–65</sup> Both physical activity and pregnancy are known to increase FGF21 myocardial expression as well. A hypothetical mechanism by which ERK1/2 and Akt activation results in increased FGF21 expression might occur by cAMP responsive binding element (CREB) transcription factor phosphorylation, which can form a binary complex with PPAR $\alpha$  which activates responsive elements in the FGF21 gene promoter, inducing its expression. Myocardial FGF21 could then be secreted into the extracellular space and bind to the cardiomyocyte membrane FGFR1c/ $\beta$ Klotho complex, activating various pathways related to cell metabolism and cytoprotection, resulting in attenuation of cardiac remodeling.<sup>56</sup>

The present study has some limitations. First, the absence of *in vitro* studies prevented us from better assessing the effects of sKlotho on FGF21 myocardial expression and confirming whether the hypothesis of modulation of FGF23 myocardial action by sKlotho is correct. Second, it would have been interesting to evaluate the expression of BNP and ANP in the heart of rKlotho-treated rats and controls, as well as inflammatory and fatty acid oxidation markers related to FGF21 actions. Finally, it would be useful to evaluate the myocardial effect of rKlotho replacement in this same experimental model with FGF21 knockout animals. However, the results support further exploration of this interaction in the future.

In conclusion, the rKlotho replacement, with a therapeutic approach, in this CKD model showed a cardioprotective effect, attenuating myocardial remodeling. This effect was associated with the reduced TRPC6 cation channel

externalization on cardiomyocyte membrane and increased myocardial FGF21 expression. This finding rises the hypothesis that  $\alpha$ Klotho replacement might interfere on FGF21 myocardial expression. Since FGF21 is a protective cardiomyokine, it could participate in  $\alpha$ Klotho-related cardioprotection, or it could be an epiphenomenon. To better explore this interaction and to deepen the understanding of the mechanisms by which this interaction would occur, *in vitro* studies with cardiomyocytes will be necessary, whereas, to evaluate the clinical effect of FGF21 deficiency and replacement in experimental CKD and uremic cardiomyopathy models, *in vivo* studies with genetically modified animals will be required.

**Authors' contributions:** PGAS, PMC, BBC, EM, MAC, JCML, MC, HP and RP contributed to the study development and procedures. PGAS wrote the manuscript. MC, HP, and RP reviewed the manuscript. All authors approved the final version of the manuscript.

#### ACKNOWLEDGEMENTS

The authors thank Dr. Marcia Koike for training in histomorphometry and Johanne Pastor for training in sKlotho measurement technique.

#### DECLARATION OF CONFLICTING INTERESTS

The author(s) declared no potential conflicts of interest with respect to the research, authorship, and/or publication of this article.


#### FUNDING

The author(s) disclosed receipt of the following financial support for the research, authorship, and/or publication of this

article: Paulo Giovanni de Albuquerque Suassuna is supported by the Fundação Instituto Mineiro de Estudos e Pesquisas em Nefrologia (IMEPEN) and Coordenação de Aperfeiçoamento de Pessoal de Nível Superior (CAPES).

#### ORCID IDs

Paulo Giovani de Albuquerque Suassuna  <https://orcid.org/0000-0002-9123-9564>

Helady Sanders-Pinheiro  <https://orcid.org/0000-0001-8603-1331>

#### REFERENCES

- Go AS. Cardiovascular disease consequences of CKD. *Semin Nephrol* 2016;**36**:293–304
- Parfrey PS, Harnett JD, Griffiths SM, Taylor R, Hand J, King A, Barre PE. The clinical course of left ventricular hypertrophy in dialysis patients. *Nephron* 1990;**55**:114–20
- Parfrey PS, Foley RN, Harnett JD, Kent GM, Murray DC, Barre PE. Outcome and risk factors for left ventricular disorders in chronic uraemia. *Nephrol Dial Transplant* 1996;**11**:1277–85
- Nik-Akhtar B, Khonsari H, Hesabi A, Khakpour M. Uremic cardiomyopathy in hemodialysis patients. *Angiology* 1978;**29**:758–63
- Alhaj E, Alhaj N, Rahman I, Niazi TO, Berkowitz R, Klapholz M. Uremic cardiomyopathy: an underdiagnosed disease. *Congest Heart Fail* 2013;**19**:E40–5
- Alpert MA. Sudden cardiac arrest and sudden cardiac death on dialysis: epidemiology, evaluation, treatment, and prevention. *Hemodial Int Symp Home Hemodial* 2011;**15**: S22–9
- de Albuquerque Suassuna PG, Sanders-Pinheiro H, de Paula RB. Uremic cardiomyopathy: a new piece in the chronic kidney disease-mineral and bone disorder puzzle. *Front Med* 2018;**5**:206
- Wang X, Shapiro JL. Evolving concepts in the pathogenesis of uraemic cardiomyopathy. *Nat Rev Nephrol* 2019;**15**:159–75
- Xie J, Wu YL, Huang CL. Deficiency of soluble alpha-Klotho as an independent cause of uremic cardiomyopathy. *Vitamins Hormones* 2016;**101**:311–30
- Kuro-O M. Klotho, phosphate and FGF-23 in ageing and disturbed mineral metabolism. *Nat Rev Nephrol* 2013;**9**:650–60
- Hu MC, Shiizaki K, Kuro-O M, Moe OW. Fibroblast growth factor 23 and klotho: physiology and pathophysiology of an endocrine network of mineral metabolism. *Annu Rev Physiol* 2013;**75**:503–33
- Faul C, Amaral AP, Oskoue B, Hu MC, Sloan A, Isakova T, Gutierrez OM, Aguillon-Prada R, Lincoln J, Hare JM, Mundel P, Morales A, Scialla J, Fischer M, Soliman EZ, Chen J, Go AS, Rosas SE, Nessel L, Townsend RR, Feldman HI, St John Sutton M, Ojo A, Gadegebeku C, Di Marco GS, Reuter S, Kentrup D, Tiemann K, Brand M, Hill JA, Moe OW, Kuro OM, Kusek JW, Keane MG, Wolf M. FGF23 induces left ventricular hypertrophy. *J Clin Invest* 2011;**121**:4393–408
- Barker SL, Pastor J, Carranza D, Quinones H, Griffith C, Goetz R, Mohammadi M, Ye J, Zhang J, Hu MC, Kuro-O M, Moe OW, Sidhu SS. The demonstration of alphaKlotho deficiency in human chronic kidney disease with a novel synthetic antibody. *Nephrol Dial Transplant* 2015;**30**:223–33
- Hu MC, Shi M, Zhang J, Addo T, Cho HJ, Barker SL, Ravikumar P, Gillings N, Bian A, Sidhu SS, Kuro-O M, Moe OW. Renal production, uptake, and handling of circulating alphaKlotho. *J Am Soc Nephrol* 2016;**27**:79–90
- Otani-Takei N, Masuda T, Akimoto T, Honma S, Watanabe Y, Shiizaki K, Miki T, Kusano E, Asano Y, Kuro OM, Nagata D. Association between serum soluble klotho levels and mortality in chronic hemodialysis patients. *Int J Endocrinol* 2015;**2015**:406269
- Kuro-O M, Matsumura Y, Aizawa H, Kawaguchi H, Suga T, Utsugi T, Ohyama Y, Kurabayashi M, Kaname T, Kume E, Iwasaki H, Iida A, Shiraki-Iida T, Nishikawa S, Nagai R, Nabeshima YI. Mutation of the mouse klotho gene leads to a syndrome resembling ageing. *Nature* 1997;**390**:45–51
- Yamamoto M, Clark JD, Pastor JV, Gurnani P, Nandi A, Kurosu H, Miyoshi M, Ogawa Y, Castrillon DH, Rosenblatt KP, Kuro-O M. Regulation of oxidative stress by the anti-aging hormone klotho. *J Biol Chem* 2005;**280**:38029–34
- Maekawa Y, Ohishi M, Ikushima M, Yamamoto K, Yasuda O, Oguro R, Yamamoto-Hanasaki H, Tataru Y, Takeya Y, Rakugi H. Klotho protein diminishes endothelial apoptosis and senescence via a mitogen-activated kinase pathway. *Geriatr Gerontol Int* 2011;**11**:510–6
- Hui H, Zhai Y, Ao L, Cleveland JC, Jr., Liu H, Fullerton DA, Meng X. Klotho suppresses the inflammatory responses and ameliorates cardiac dysfunction in aging endotoxemic mice. *Oncotarget* 2017;**8**:15663–76
- Hu MC, Shi M, Cho HJ, Adams-Huet B, Paek J, Hill K, Shelton J, Amaral AP, Faul C, Taniguchi M, Wolf M, Brand M, Takahashi M, Kuro OM, Hill JA, Moe OW. Klotho and phosphate are modulators of pathologic uremic cardiac remodeling. *J Am Soc Nephrol* 2015;**26**:1290–302
- Xie J, Yoon J, An SW, Kuro-O M, Huang CL. Soluble klotho protects against uremic cardiomyopathy independently of fibroblast growth factor 23 and phosphate. *J Am Soc Nephrol* 2015;**26**:1150–60
- Xie J, Cha SK, An SW, Kuro OM, Birnbaumer L, Huang CL. Cardioprotection by klotho through downregulation of TRPC6 channels in the mouse heart. *Nat Commun* 2012;**3**:1238
- Chen G, Liu Y, Goetz R, Fu L, Jayaraman S, Hu MC, Moe OW, Liang G, Li X, Mohammadi M. alpha-Klotho is a non-enzymatic molecular scaffold for FGF23 hormone signalling. *Nature* 2018;**553**:461–6
- Richter B, Faul C. FGF23 actions on target tissues-with and without klotho. *Front Endocrinol* 2018;**9**:189
- Adams AC, Cheng CC, Coskun T, Kharitonov A. FGF21 requires betaklotho to act in vivo. *PLoS One* 2012;**7**:e49977
- Kharitonov A, Shyanova TL, Koester A, Ford AM, Micanovic R, Galbreath EJ, Sandusky GE, Hammond LJ, Moyers JS, Owens RA, Gromada J, Brozinick JT, Hawkins ED, Wroblewski VJ, Li DS, Mehrbod F, Jaskunas SR, Shanafelt AB. FGF-21 as a novel metabolic regulator. *J Clin Invest* 2005;**115**:1627–35
- Joki Y, Ohashi K, Yuasa D, Shibata R, Ito M, Matsuo K, Kambara T, Uemura Y, Hayakawa S, Hiramatsu-Ito M, Kanemura N, Ogawa H, Daida H, Murohara T, Ouchi N. FGF21 attenuates pathological myocardial remodeling following myocardial infarction through the adiponectin-dependent mechanism. *Biochem Biophys Res Commun* 2015;**459**:124–30
- Redondo-Angulo I, Mas-Stachurska A, Sitges M, Tinahones FJ, Giralt M, Villarroya F, Planavila A. Fgf21 is required for cardiac remodeling in pregnancy. *Cardiovasc Res* 2017;**113**:1574–84
- Feingold KR, Grunfeld C, Heuer JG, Gupta A, Cramer M, Zhang T, Shigenaga JK, Patzek SM, Chan ZW, Moser A, Bina H, Kharitonov A. FGF21 is increased by inflammatory stimuli and protects leptin-deficient ob/ob mice from the toxicity of sepsis. *Endocrinology* 2012;**153**:2689–700
- Desai BN, Singhal G, Watanabe M, Stevanovic D, Lundasen T, Fisher FM, Mather ML, Vardeh HG, Douris N, Adams AC, Nasser IA, FitzGerald GA, Flier JS, Skarke C, Maratos-Flier E. Fibroblast growth factor 21 (FGF21) is robustly induced by ethanol and has a protective role in ethanol associated liver injury. *Mol Metab* 2017;**6**:1395–406
- Xu J, Lloyd DJ, Hale C, Stanislaus S, Chen M, Sivits G, Vonderfecht S, Hecht R, Li YS, Lindberg RA, Chen JL, Jung DY, Zhang Z, Ko HJ, Kim JK, Veniant MM. Fibroblast growth factor 21 reverses hepatic steatosis, increases energy expenditure, and improves insulin sensitivity in diet-induced obese mice. *Diabetes* 2009;**58**:250–9
- Suomalainen A. Fibroblast growth factor 21: a novel biomarker for human muscle-manifesting mitochondrial disorders. *Expert Opin Med Diagn* 2013;**7**:313–7
- Luo Y, Ye S, Chen X, Gong F, Lu W, Li X. Rush to the fire: FGF21 extinguishes metabolic stress, metaflammation and tissue damage. *Cytokine Growth Factor Rev* 2017;**38**:59–65
- Liang P, Zhong L, Gong L, Wang J, Zhu Y, Liu W, Yang J. Fibroblast growth factor 21 protects rat cardiomyocytes from endoplasmic reticulum stress by promoting the fibroblast growth factor receptor

- 1-extracellular signal-regulated kinase 1/2 signaling pathway. *Int J Mol Med* 2017;**40**:1477–85
35. Planavila A, Redondo-Angulo I, Ribas F, Garrabou G, Casademont J, Giralt M, Villarroya F. Fibroblast growth factor 21 protects the heart from oxidative stress. *Cardiovasc Res* 2015;**106**:19–31
36. Planavila A, Redondo I, Hondares E, Vinciguerra M, Munts C, Iglesias R, Gabrielli LA, Sitges M, Giralt M, van Bilsen M, Villarroya F. Fibroblast growth factor 21 protects against cardiac hypertrophy in mice. *Nat Commun* 2013;**4**:2019
37. Ormrod D, Miller T. Experimental uremia. Description of a model producing varying degrees of stable uremia. *Nephron* 1980;**26**:249–54
38. Doi S, Zou Y, Togao O, Pastor JV, John GB, Wang L, Shiizaki K, Gotschall R, Schiavi S, Yorioka N, Takahashi M, Boothman DA, Kuro-o M. Klotho inhibits transforming growth factor-beta1 (TGF-beta1) signaling and suppresses renal fibrosis and cancer metastasis in mice. *J Biol Chem* 2011;**286**:8655–65
39. Robinson LA, Braimbridge MV, Hearse DJ. Comparison of the protective properties of four clinical crystalloid cardioplegic solutions in the rat heart. *Ann Thorac Surg* 1984;**38**:268–74
40. Custodio MR, Koike MK, Neves KR, dos Reis LM, Gracioli FG, Neves CL, Batista DG, Magalhaes AO, Hawlitschek P, Oliveira IB, Dominguez WV, Moyses RM, Jorgetti V. Parathyroid hormone and phosphorus overload in uremia: impact on cardiovascular system. *Nephrol Dial Transplant* 2012;**27**:1437–45
41. Helps SC, Thornton E, Kleinig TJ, Manavis J, Vink R. Automatic non-subjective estimation of antigen content visualized by immunohistochemistry using color deconvolution. *Appl Immunohistochem Mol Morphol* 2012;**20**:82–90
42. Maquigussa E, Paterno JC, de Oliveira Pokorny GH, da Silva Perez M, Varela VA, da Silva Novaes A, Schor N, Boim MA. Klotho and PPAR gamma activation mediate the renoprotective effect of losartan in the 5/6 nephrectomy model. *Front Physiol* 2018;**9**:1033
43. Romero-Calvo I, Ocon B, Martinez-Moya P, Suarez MD, Zarzuelo A, Martinez-Augustin O, de Medina FS. Reversible ponceau staining as a loading control alternative to actin in Western blots. *Anal Biochem* 2010;**401**:318–20
44. Henao Agudelo JS, Braga TT, Amano MT, Cenedeze MA, Cavinato RA, Peixoto-Santos AR, Muscara MN, Teixeira SA, Cruz MC, Castoldi A, Sinigaglia-Coimbra R, Pacheco-Silva A, de Almeida DC, Camara N. Mesenchymal stromal Cell-Derived microvesicles regulate an internal Pro-Inflammatory program in activated macrophages. *Front Immunol* 2017;**8**:881
45. Livak KJ, Schmittgen TD. Analysis of relative gene expression data using real-time quantitative PCR and the 2(-Delta Delta C(T)) method. *Methods* 2001;**25**:402–8
46. Song S, Gao P, Xiao H, Xu Y, Si LY. Klotho suppresses cardiomyocyte apoptosis in mice with stress-induced cardiac injury via downregulation of endoplasmic reticulum stress. *PLoS One* 2013;**8**:e82968
47. Yu L, Meng W, Ding J, Cheng M. Klotho inhibits angiotensin II-induced cardiomyocyte hypertrophy through suppression of the AT1R/beta catenin pathway. *Biochem Biophys Res Commun* 2016;**473**:455–61
48. Yang K, Wang C, Nie L, Zhao X, Gu J, Guan X, Wang S, Xiao T, Xu X, He T, Xia X, Wang J, Zhao J. Klotho protects against indoxyl Sulphate-Induced myocardial hypertrophy. *J Am Soc Nephrol* 2015;**26**:2434–46
49. McDonald TA, Zepeda ML, Tomlinson MJ, Bee WH, Ivens IA. Subcutaneous administration of biotherapeutics: current experience in animal models. *Curr Opin Mol Ther* 2010;**12**:461–70
50. Bush EW, Hood DB, Papst PJ, Chapo JA, Minobe W, Bristow MR, Olson EN, McKinsey TA. Canonical transient receptor potential channels promote cardiomyocyte hypertrophy through activation of calcineurin signaling. *J Biol Chem* 2006;**281**:33487–96
51. Wu X, Eder P, Chang B, Molkentin JD. TRPC channels are necessary mediators of pathologic cardiac hypertrophy. *Proc Natl Acad Sci U S A* 2010;**107**:7000–5
52. Eder P, Molkentin JD. TRPC channels as effectors of cardiac hypertrophy. *Circ Res* 2011;**108**:265–72
53. Dalton G, An SW, Al-Juboori SI, Nischan N, Yoon J, Dobrinskikh E, Hilgemann DW, Xie J, Luby-Phelps K, Kohler JJ, Birnbaumer L, Huang CL. Soluble klotho binds monosialoganglioside to regulate membrane microdomains and growth factor signaling. *Proc Natl Acad Sci U S A* 2017;**114**:752–7
54. Kim KH, Lee MS. FGF21 as a stress hormone: the roles of FGF21 in stress adaptation and the treatment of metabolic diseases. *Diabetes Metab J* 2014;**38**:245–51
55. Salminen A, Kaarniranta K, Kauppinen A. Integrated stress response stimulates FGF21 expression: systemic enhancer of longevity. *Cell Signal* 2017;**40**:10–21
56. Wang S, Wang Y, Zhang Z, Liu Q, Gu J. Cardioprotective effects of fibroblast growth factor 21 against doxorubicin-induced toxicity via the SIRT1/LKB1/AMPK pathway. *Cell Death Dis* 2017;**8**:e3018
57. Ravikumar P, Ye J, Zhang J, Pinch SN, Hu MC, Kuro-O M, Hsia CC, Moe OW. Alpha-Klotho protects against oxidative damage in pulmonary epithelia. *Am J Physiol Lung Cell Mol Physiol* 2014;**307**:L566–75
58. Rizzo B, Maltese G, Paraskevi MP, Hrelia S, Mann G, Siow R. Induction of antioxidant genes by sulforaphane and klotho in human aortic smooth muscle cells. *Free Radic Biol Med* 2014;**75**:S14–5
59. Buendia P, Ramirez R, Aljama P, Carracedo J. Klotho prevents translocation of NFkappaB. *Vit Hormones* 2016;**101**:119–50
60. Mytych J, Solek P, Koziorowski M. Klotho modulates ER-mediated signaling crosstalk between prosurvival autophagy and apoptotic cell death during LPS challenge. *Apoptosis* 2018;**24**:95–107
61. Stein S, Bachmann A, Lossner U, Kratzsch J, Bluher M, Stumvoll M, Fasshauer M. Serum levels of the adipokine FGF21 depend on renal function. *Diab Care* 2009;**32**:126–8
62. Lin Z, Zhou Z, Liu Y, Gong Q, Yan X, Xiao J, Wang X, Lin S, Feng W, Li X. Circulating FGF21 levels are progressively increased from the early to end stages of chronic kidney diseases and are associated with renal function in Chinese. *PLoS One* 2011;**6**:e18398
63. Ellison GM, Waring CD, Vicinanza C, Torella D. Physiological cardiac remodelling in response to endurance exercise training: cellular and molecular mechanisms. *Heart* 2012;**98**:5–10
64. Li J, Umar S, Amjadi M, Iorga A, Sharma S, Nadadur RD, Regitz-Zagrosek V, Eghbali M. New frontiers in heart hypertrophy during pregnancy. *Am J Cardiovasc Dis* 2012;**2**:192–207
65. Shimizu I, Minamino T. Physiological and pathological cardiac hypertrophy. *J Mol Cell Cardiol* 2016;**97**:245–62

(Received July 27, 2019, Accepted November 21, 2019)